

A Numerical Study for the Homogenization of One-Dimensional Models describing the Motion of Dislocations

A. Ghorbel*, P. Hoch[†], R. Monneau*

Abstract

In this paper we are interested in the collective motion of dislocations defects in crystals. Mathematically we study the homogenization of a non-local Hamilton-Jacobi equation. We prove some qualitative properties on the effective hamiltonian. We also provide a numerical scheme which is proved to be monotone under some suitable CFL conditions. Using this scheme, we compute numerically the effective hamiltonian. Furthermore we also provide numerical computations of the effective hamiltonian for several models corresponding to the dynamics of dislocations where no theoretical analysis is available.

AMS Classification: 35B27, 35F20, 35F25, 35K55, 49L25, 65N06, 65N12, 74N05.

Keywords: continuous viscosity solution, Dislocations dynamics, eikonal equation, effective hamiltonian, finite difference scheme, Hamilton-Jacobi equation, non-local equation, numerical homogenization, Peach-Koehler force, transport equation.

1 Introduction

In this paper we study the homogenization of non-local Hamilton-Jacobi equations modelling dislocations dynamics, we propose a scheme and provide numerical simulations for several models.

1.1 Physical modelling of dislocations dynamics

In this work, we are interested in the collective behaviour of several dislocations moving in a crystal. Dislocations are defects present in real crystals and are at the origin of the plastic behaviour of metals. We refer to [11] for a physical description of dislocations.

In our work and in the simplest case, we consider a particular geometry of parallel dislocations lines moving in the same plane. This particular geometry can be modeled by a 1D problem where the position of the dislocations is given by the point $x \in \mathbb{R}$ where a function $u(x, t)$ takes integer values. In the simplest case, we assume that u satisfies the following non-local Hamilton-Jacobi equation (see [9] and [12] for a study of a similar model)

$$\begin{cases} \frac{\partial u}{\partial t}(x, t) = c[u](x, t) \left| \frac{\partial u}{\partial x}(x, t) \right| & \text{in } \mathbb{R} \times (0, +\infty) \\ c[u](x, t) = A + c^1(x) + c^{\text{int}}[u](x, t) \\ c^{\text{int}}[u](x, t) = \int_{\mathbb{R}} c^0(x') u(x - x', t) dx' \end{cases} \quad (1)$$

¹CERMICS, École Nationale des Ponts et Chaussées, 6 et 8 avenue Blaise Pascal, Cité Descartes, Champs-sur-Marne, 77455 Marne-la-Vallée Cedex 2.

²CEA/DAM Ile de France, Service DCSA/SSEL, BP 12, 91680 Bruyères Le Chatel.

with initial condition

$$u(x, 0) = u_0(x) \quad \text{on } \mathbb{R} \quad (2)$$

Here $c[u]$ denotes the velocity of the dislocations. It is the sum of three terms: c^{int} is the contribution created by the interactions with all the dislocations, and is given by a convolution, c^1 is a microscopic field created by the other defects in the crystal and $A \in \mathbb{R}$ is the exterior applied stress.

We will study problem (1) and similar equations in the framework of viscosity solutions. Let us recall that the notion of viscosity solution was first introduced by Crandall and Lions in [5] for first order Hamilton-Jacobi equations. For an introduction to this notion, see in particular the books of Barles [4], and of Bardi and Capuzzo-Dolcetta [3], and the User's guide of Crandall, Ishii and Lions [6].

We assume that the kernel c^0 satisfies

$$c^0(x) = c^0(-x) \text{ and } \int_{\mathbb{R}} c^0(x) dx = 0. \quad (3)$$

We also assume the periodicity and the regularity of the micro-stress c^1

$$c^1(x+1) = c^1(x) \quad \text{on } \mathbb{R}, \quad \text{and} \quad c^1 \text{ is Lipschitz-continuous} \quad (4)$$

1.2 Goal of the paper

We want to understand the properties of the solutions of (1) for $A = 0$ at a large scale defining

$$u^\varepsilon(x, t) = \varepsilon u\left(\frac{x}{\varepsilon}, \frac{t}{\varepsilon}\right)$$

where ε is the ratio between the mesoscopic scale and the microscopic scale associated to dislocations (like distances between obstacles to the motion of dislocations).

Homogenization of Hamilton-Jacobi Equations was studied by Lions, Papanicolaou and Varadhan in [14] and this work was followed by a large literature on the subject, that would be difficult to cite here.

For this equation (see [12]) and for a certain class of kernels c^0 , it is known that u^ε converges to u^0 , solution of

$$\frac{\partial u^0}{\partial t} = \bar{H}\left(I_1 u^0, \frac{\partial u^0}{\partial x}\right)$$

where I_1 is a non-local Levy operator, and \bar{H} is the effective hamiltonian given by the following definition.

Definition 1.1 (Effective hamiltonian)

We assume (4). For $(A, p) \in \mathbb{R} \times \mathbb{R}$, the effective hamiltonian $\bar{H}(A, p)$ is defined by

$$\bar{H}(A, p) = \lim_{t \rightarrow +\infty} \frac{w(x, t)}{t} \quad (\text{independent on } x) \quad (5)$$

where w solves the "cell problem", i.e. w solves (1) with $w(x, 0) = px$.

Then the goal of the present paper is to compute numerically $\bar{H}(A, p)$ for equation (1) for specific kernels c^0 . In particular, we numerically check that the ergodicity property (5) holds for general kernels c^0 (like for instance for the Peierls-Nabarro model, see subsection 5.2), even in the case where the equation has no comparison principle and it is even not clear if (5) holds theoretically. We also do some simulations for some similar equations or systems of equations. To this end, we implemented several numerical schemes.

1.3 Brief presentation of our results

We present here properties of the effective hamiltonian and the scheme used to compute it numerically. We prove the following qualitative result on the effective hamiltonian.

Theorem 1.1 (Monotonicity of the effective hamiltonian)

For the choice $c^0 = -\delta_0 + J$ with δ_0 is a Dirac mass and $J \in C^\infty(\mathbb{R})$ is such that

$$\begin{cases} J(-x) = J(x) \geq 0 & ; \quad \int_{\mathbb{R}} J(x) dx = 1 \quad \text{and} \quad \int_{\mathbb{R}} |x| J(x) dx < +\infty \\ c_2 := \inf_{\delta \in [0,1]} \int_{\mathbb{R}} \min(J(z), J(z+\delta)) dz > 0 \end{cases} \quad (6)$$

Then the effective hamiltonian given in Definition 1.1 satisfies

1. $\bar{H}(A, p)$ is non-decreasing in A .
2. If $\int_{\mathbb{R}} c^1(x) dx = 0$ then $\bar{H}(0, p) = 0$ and $A\bar{H}(A, p)$ is non-decreasing in $|p|$ and satisfies

$$\text{sgn}(A) \left(|A| + 1 + \frac{2}{c_2} \right) \geq \text{sgn}(A) \frac{\partial \bar{H}}{\partial |p|}(A, p) \geq 0.$$

We build a finite difference scheme of order one in space and time using an explicit Euler scheme in time and an upwind scheme in space. Given a mesh size Δx , Δt and a lattice $I_d = \{(i\Delta x, n\Delta t); i \in \mathbb{Z}, n \in \mathbb{N}\}$, (x_i, t_n) denotes the node $(i\Delta x, n\Delta t)$ and $v^n = (v_i^n)_i$ the values of the numerical approximation of the continuous solution $u(x_i, t_n)$. We then consider the following numerical scheme:

$$v_i^0 = u_0(x_i), \quad v_i^{n+1} = v_i^n + \Delta t c_i(v^n) \times \begin{cases} D_x^+ v_i^n & \text{if } c_i(v^n) \geq 0 \\ D_x^- v_i^n & \text{if } c_i(v^n) < 0 \end{cases} \quad (7)$$

with $D_x^- v_i^n = \frac{v_i^n - v_{i-1}^n}{\Delta x}$ and $D_x^+ v_i^n = \frac{v_{i+1}^n - v_i^n}{\Delta x}$. The discrete velocity is

$$c_i(v^n) = A + c^1(x_i) + c_i^{\text{int}}(v^n) \quad (8)$$

We approximate the non-local term $c^0 \star u$ by

$$\begin{cases} c_i^{\text{int}}(v^n) = -v_i^n + \sum_{l \in \mathbb{Z}} J_l v_{i-l}^n \Delta x \\ J_i = \frac{1}{\Delta x} \int_{I_i} J(x) dx \quad \text{and} \quad I_i = \left[x_i - \frac{\Delta x}{2}, x_i + \frac{\Delta x}{2} \right]. \end{cases} \quad (9)$$

Several works have been done for the discretization of more general first order Hamilton-Jacobi equations (even with boundary conditions). We refer in particular to the work of Abgrall [1].

Then we have the following result about monotonicity of the scheme (7) for the special kernel $c^0 = -\delta_0 + J$.

Theorem 1.2 (Monotonicity of the scheme)

We assume that

$$v_{i+1}^0 \geq v_i^0, \quad \forall i \in \mathbb{Z} \quad (10)$$

$$(\text{respectively } w_{i+1}^0 \geq w_i^0, \quad \forall i \in \mathbb{Z}) \quad (11)$$

If the time step Δt satisfies

$$\Delta t \leq \left(\sup_{j \in \mathbb{Z}} \frac{|c_{j+1}(v^k) - c_j(v^k)|}{\Delta x} \right)^{-1}, \quad \text{for } 0 \leq k \leq n \quad (12)$$

$$(\text{respectively } \Delta t \leq \left(\sup_{j \in \mathbb{Z}} \frac{|c_{j+1}(w^k) - c_j(w^k)|}{\Delta x} \right)^{-1}, \quad \text{for } 0 \leq k \leq n) \quad (13)$$

Then we have the monotonicity preservation:

$$v_{i+1}^k \geq v_i^k, \quad \forall i \in \mathbb{Z}, \quad \forall 0 \leq k \leq n+1 \quad (14)$$

$$(\text{respectively } w_{i+1}^k \geq w_i^k, \quad \forall i \in \mathbb{Z}, \quad \forall 0 \leq k \leq n+1) \quad (15)$$

Assume moreover that

$$v_i^0 \geq w_i^0, \quad \forall i \in \mathbb{Z}. \quad (16)$$

If the time step Δt satisfies moreover

$$\Delta t \sup_{j \in \mathbb{Z}} \left\{ \max \left(\frac{v_{j+1}^k - v_j^k}{\Delta x}, \frac{w_{j+1}^k - w_j^k}{\Delta x} \right) \right\} \leq \frac{1}{2} \quad \text{for } 0 \leq k \leq n \quad (17)$$

and

$$\frac{\Delta t}{\Delta x} \leq \frac{1}{2} \left(\sup_{j \in \mathbb{Z}} \left\{ \max \left(|c_j(v^k)|, |c_j(w^k)| \right) \right\} \right)^{-1} \quad \text{for } 0 \leq k \leq n \quad (18)$$

Then

$$v_i^k \geq w_i^k, \quad \forall i \in \mathbb{Z} \quad \text{for } 0 \leq k \leq n+1. \quad (19)$$

Remark 1.1 *There would be no monotonicity of the scheme if J would be negative.*

We use this scheme to compute numerically an approximation $\bar{H}^{\text{num}}(A, p)$ of $\bar{H}(A, p)$. We numerically check that $\bar{H}^{\text{num}}(A, p)$ satisfies the monotonicity properties given in Theorem 1.1. We also compute the effective hamiltonian for other similar equations (like for instance the case with Peierls-Nabarro kernel, see subsection 5.2), and for some systems of equations (see Section 6).

There are very few works on numerics for homogenization. Up to our knowledge, let us mention for convex first order hamiltonians the work of Gomes and Oberman [10] computing the effective hamiltonian using a variational approach and the work of Rorro [15] using semi-Lagrangian schemes.

1.4 Organization of the paper

In Section 2, we give the proof of Theorem 1.1. In Section 3, we study the numerical scheme and prove Theorem 1.2. In Section 4, we give numerical simulations corresponding to the scheme of Theorem 1.2. In Section 5, we present numerical simulations for similar equations with for instance the Peierls-Nabarro kernel. In Section 6, we present numerical simulations for systems of equations for two types of dislocations. Finally in the Appendix we provide the proof of a technical Lemma (Lemma 2.1) and give a brief derivation of the kernel for walls of dislocations.

2 Qualitative properties of the effective hamiltonian

Before to prove Theorem 1.1, we need the following lemma with the proof given in the Appendix.

Lemma 2.1 (Coercivity of the convolution)

Assume J satisfies (6) and $c^0 = -\delta_0 + J$. If $u \in C_b^0(\mathbb{R})$ is maximal at $Y \in \mathbb{R}$ and minimal at $y \in \mathbb{R}$ and $|Y - y| < 1$ then

$$(c^0 \star u)(Y) - (c^0 \star u)(y) \leq -c_2 (u(Y) - u(y))$$

To keep light notation, we denote in this section by M the operator such that

$$(Mv)(x) = (c^0 \star v)(x) = -v(x) + \int_{\mathbb{R}} J(z)v(x-z) dz. \quad (20)$$

We will also need the following result.

Lemma 2.2 (Existence of sub and supercorrectors)

For any $p \in \mathbb{R}$ and $A \in \mathbb{R}$, there exist $\lambda \in \mathbb{R}$, a subcorrector $\underline{v}(x)$ and a supercorrector $\bar{v}(x)$ which are 1-periodic in x and satisfy

$$\begin{aligned} \lambda &\leq |p + \partial_x \underline{v}| (c^1 + A + M\underline{v}), \quad \text{with } p(p + \partial_x \underline{v}) \geq 0 \quad \text{on } \mathbb{R} \\ \lambda &\geq |p + \partial_x \bar{v}| (c^1 + A + M\bar{v}), \quad \text{with } p(p + \partial_x \bar{v}) \geq 0 \quad \text{on } \mathbb{R} \end{aligned}$$

with

$$\max \underline{v} - \min \underline{v} \leq \frac{2}{c_2} |c^1|_{L^\infty(\mathbb{R})} \quad \text{and} \quad \max \bar{v} - \min \bar{v} \leq \frac{2}{c_2} |c^1|_{L^\infty(\mathbb{R})}$$

where c_2 given in (6).

The proof of Lemma 2.2 is a slight adaptation of the work [12]. We give below a quick proof of this fact.

SKETCH OF THE PROOF OF LEMMA 2.2

Let us work in the case $p > 0$ (the case $p < 0$ is similar, and for the case $p = 0$, we have $\lambda = 0$ with a corrector equal to zero).

Step 1

Using the theory developed in [12], let us start to consider (using the fact that $\int_{\mathbb{R}} |x| J(x) dx < +\infty$), for $p > 0$, the solution u of

$$\begin{cases} u_t = |\partial_x u| (c^1 + A + M(u - p \cdot)) \\ u(x, t = 0) = px \end{cases}$$

then $\bar{\omega}(t) = \inf_x \partial_x u(t, x)$ formally satisfies

$$\bar{\omega}_t \geq |\bar{\omega}| (\partial_x c^1 + M\bar{\omega}) \geq |\bar{\omega}| (\partial_x c^1) \quad \text{with } \bar{\omega}(0) = p > 0$$

and therefore the bound from below on the possible exponential decay of $\bar{\omega}$ implies that

$$\partial_x u \geq 0$$

This result can be justified rigorously using some classical viscosity arguments (as in [12]). We also know that $u(t, x) - px$ is 1-periodic in x . We already know by [12] that there exists a unique $\lambda \in \mathbb{R}$ such that $v(t, x) = u(t, x) - px - \lambda t$ is bounded. Moreover $\lambda = \bar{H}(A, p)$. Let us now define Y_t and

y_t such that $M(t) := \max_x v(t, x) = v(t, Y_t)$ and $m(t) := \min_x v(t, x) = v(t, y_t)$ and $|Y_t - y_t| < 1$, we get formally

$$\begin{aligned}\lambda + M'(t) &\leq |p| (c^1(Y_t) + A + (Mv)(Y_t)) \\ \lambda + m'(t) &\geq |p| (c^1(y_t) + A + (Mv)(y_t))\end{aligned}$$

which implies for $p \neq 0$ that $\omega(t) = M(t) - m(t)$ satisfies

$$\omega'(t)/|p| - ((Mv)(Y_t) - (Mv)(y_t)) \leq c^1(Y_t) - c^1(y_t)$$

And then by Lemma 2.1, we get that

$$\omega'(t)/|p| + c_2\omega(t) \leq c^1(Y_t) - c^1(y_t) \quad \text{with} \quad \omega(0) = 0.$$

This inequality can be justified rigorously by routine viscosity arguments. We deduce that for every $t \geq 0$

$$\omega(t) = \max_x v(t, x) - \min_x v(t, x) \leq \frac{2}{c_2} |c^1|_{L^\infty(\mathbb{R})}$$

Step 2

Considering the semi-relaxed limits of $u(t, x) - px - \lambda t$ with the supremum (resp. the infimum) in time, we build a subsolution \underline{v} (resp. a supersolution \bar{v}) of the following equation

$$\lambda = |p + \partial_x v| (c^1 + A + Mv)$$

which satisfies the expected properties.

This ends the proof of the Lemma. □

PROOF OF THEOREM 1.1

- 1) We first prove the monotonicity of $\bar{H}(A, p)$ in A . Let us consider $A_2 > A_1$, $\lambda_i = \bar{H}(A_i, p)$, $i = 1, 2$ and a subcorrector \underline{v}_1 for (A, p) then we have

$$\begin{aligned}\lambda_1 &\leq |p + \partial_x \underline{v}_1| (c^1 + A_1 + M\underline{v}_1) \\ &\leq |p + \partial_x \underline{v}_1| (c^1 + A_2 + M\underline{v}_1)\end{aligned}$$

This shows $\underline{v}_1(x) + px + \lambda_1 t$ is a subsolution to the cell problem which implies that $\lambda_2 \geq \lambda_1$ i.e. $\bar{H}(A_2, p) \geq \bar{H}(A_1, p)$.

- 2) We now prove that $\bar{H}(0, p) = 0$ in the case $\int_{(0,1)} c^1 = 0$. Let us define v_0 as the periodic solution of

$$Mv_0 = -c^1 \quad \text{on } \mathbb{R} \tag{21}$$

such that $\int_{(0,1)} v_0 = 0$. We see that v_0 is a corrector for the cell problem with $\lambda = 0 = \bar{H}(0, p)$.

- 3) Let us now show the monotonicity in $|p|$ in the case $\int_{(0,1)} c^1 = 0$. For $p_2 > p_1 > 0$ and $A > 0$ such that $\lambda_1 > 0$ with $\lambda_i = \bar{H}(A, p_i)$, $i = 1, 2$ (the other cases are similar), let us consider a subcorrector \underline{v}_1 satisfying

$$0 < \lambda_1 \leq (p_1 + \partial_x \underline{v}_1) (c^1 + A + M\underline{v}_1) \quad \text{with} \quad p_1 + \partial_x \underline{v}_1 \geq 0$$

and a supercorrector \bar{v}_1 satisfying

$$\lambda_1 \geq (p_1 + \partial_x \bar{v}_1) (c^1 + A + M\bar{v}_1) \quad \text{with} \quad p_1 + \partial_x \bar{v}_1 \geq 0$$

From Lemma 2.2, we also know that we can bound these sub/supercorrectors by $\frac{2}{c_2} |c^1|_{L^\infty(\mathbb{R})}$. Therefore

$$0 \leq c^1 + A + M\underline{v}_1 \quad \text{and} \quad \left(1 + \frac{2}{c_2}\right) |c^1|_{L^\infty(\mathbb{R})} \geq c^1 + M\underline{v}_1.$$

And then

$$\lambda_1 \leq \lambda_1 + (p_2 - p_1) (c^1 + A + M\underline{v}_1) \leq (p_2 + \partial_x \underline{v}_1) (c^1 + A + M\underline{v}_1)$$

which implies $\lambda_2 \geq \lambda_1 > 0$.

Similarly, we have

$$\begin{aligned} \lambda_1 + \left(\left(1 + \frac{2}{c_2}\right) |c^1|_{L^\infty(\mathbb{R})} + A \right) (p_2 - p_1) &\geq \lambda_1 + (p_2 - p_1) (c^1 + A + M\bar{v}_1) \\ &\geq (p_2 + \partial_x \bar{v}_1) (c^1 + A + M\bar{v}_1) \end{aligned}$$

which implies $\lambda_2 \leq \lambda_1 + \left(\left(1 + \frac{2}{c_2}\right) |c^1|_{L^\infty(\mathbb{R})} + A \right) (p_2 - p_1)$ and gives the result. \square

3 Monotonicity of the scheme

In this section we prove Theorem 1.2 . We will use the following result (consequence of Lemma 2.5.2 in [9])

Lemma 3.1 (A monotonicity preserving scheme for prescribed velocity)

We assume that

$$v_i^{n+1} = v_i^n + \frac{\Delta t}{\Delta x} c_i^n \times \begin{cases} v_{i+1}^n - v_i^n & \text{if } c_i^n \geq 0 \\ v_i^n - v_{i-1}^n & \text{if } c_i^n < 0 \end{cases}$$

and

$$\Delta t \leq \frac{1}{2} \left(\sup_{j \in \mathbb{Z}} \frac{|c_{j+1}^k - c_j^k|}{\Delta x} \right)^{-1} \quad \text{for } 0 \leq k \leq n \quad (22)$$

If

$$v_{i+1}^0 \geq v_i^0, \quad \forall i \in \mathbb{Z}$$

then

$$v_{i+1}^k \geq v_i^k, \quad \forall i \in \mathbb{Z}, \quad \text{for } 0 \leq k \leq n+1.$$

PROOF OF THEOREM 1.2

Let $(v_i^n)_{i \in \mathbb{Z}, n \in \mathbb{N}}$ and $(w_i^n)_{i \in \mathbb{Z}, n \in \mathbb{N}}$ two discrete solutions, such that v_i^0 and w_i^0 are non-decreasing in $i \in \mathbb{Z}$. We set $M^n(v) := \sup_{i \in \mathbb{Z}} \frac{v_{i+1}^n - v_i^n}{\Delta x}$ and $M^n(w) := \sup_{i \in \mathbb{Z}} \frac{w_{i+1}^n - w_i^n}{\Delta x}$. One write the numerical

scheme for v (and the same for w)

$$v_i^{n+1} = v_i^n + \frac{\Delta t}{\Delta x} c_i(v^n) \times \begin{cases} v_{i+1}^n - v_i^n & \text{if } c_i(v^n) \geq 0 \\ v_i^n - v_{i-1}^n & \text{if } c_i(v^n) < 0 \end{cases} \quad (23)$$

with $c_i(v^n)$ defined in (8)-(9). Let us assume that $v_i^k \geq w_i^k$, $\forall i \in \mathbb{Z}, \forall 0 \leq k \leq n$. Let us prove that it is still true for $k = n + 1$.

Case 1: We assume that $c_i(v^n) \geq 0$ and $c_i(w^n) \geq 0$.

We have

$$v_i^{n+1} - w_i^{n+1} = v_i^n - w_i^n + \frac{\Delta t}{\Delta x} (c_i(v^n) (v_{i+1}^n - v_i^n) - c_i(w^n) (w_{i+1}^n - w_i^n)).$$

One can add and subtract $\frac{\Delta t}{\Delta x} c_i(w^n) (v_{i+1}^n - v_i^n)$, and one obtains

$$\begin{aligned} v_i^{n+1} - w_i^{n+1} &= (v_i^n - w_i^n) \left(1 - \frac{\Delta t}{\Delta x} c_i(w^n) \right) + \frac{\Delta t}{\Delta x} c_i(w^n) (v_{i+1}^n - w_{i+1}^n) \\ &\quad + \frac{\Delta t}{\Delta x} (c_i(v^n) - c_i(w^n)) (v_{i+1}^n - v_i^n) \\ &\geq (v_i^n - w_i^n) \left(1 - \frac{\Delta t}{\Delta x} c_i(w^n) \right) + \frac{\Delta t}{\Delta x} (c_i(v^n) - c_i(w^n)) (v_{i+1}^n - v_i^n) \end{aligned}$$

where we have used the fact that $v_{i+1}^n \geq w_{i+1}^n$. Since

$$c_i(v^n) = A + c^1(x_i) - v_i^n + \sum_{j \in \mathbb{Z}} J_j v_{i-j}^n \Delta x \quad (24)$$

the difference between the discrete velocities can be written as

$$c_i(v^n) - c_i(w^n) = -(v_i^n - w_i^n) + \sum_{j \in \mathbb{Z}} J_j (v_{i-j}^n - w_{i-j}^n) \Delta x \quad (25)$$

and then we get (using $J_j \geq 0$ and $v_{i-j}^n - w_{i-j}^n \geq 0$)

$$\begin{aligned} v_i^{n+1} - w_i^{n+1} &\geq (v_i^n - w_i^n) \left(1 - \frac{\Delta t}{\Delta x} c_i(w^n) \right) - \frac{\Delta t}{\Delta x} (v_i^n - w_i^n) (v_{i+1}^n - v_i^n) \\ &\geq (v_i^n - w_i^n) \left(1 - \frac{\Delta t}{\Delta x} c_i(w^n) - M^n(u) \Delta t \right) \end{aligned} \quad (26)$$

Therefore we have

$$v_i^{n+1} - w_i^{n+1} \geq (v_i^n - w_i^n) \left(1 - \frac{\Delta t}{\Delta x} c_i(w^n) - M^n(u) \Delta t \right). \quad (27)$$

It is then sufficient to have the following two restrictions on the time step

$$\frac{\Delta t}{\Delta x} \leq \left(2 \sup_{j \in \mathbb{Z}} |c_j(v^n)| \right)^{-1} \quad \text{and} \quad M^n(u) \Delta t \leq \frac{1}{2}$$

to deduce that the scheme is monotone in this case.

Case 2: We assume that $c_i(v^n) \leq 0$ and $c_i(w^n) \leq 0$.

We compute

$$v_i^{n+1} - w_i^{n+1} = v_i^n - w_i^n + \frac{\Delta t}{\Delta x} c_i(v^n)(v_i^n - v_{i-1}^n) - \frac{\Delta t}{\Delta x} c_i(w^n)(w_i^n - w_{i-1}^n).$$

One can add and subtract $\frac{\Delta t}{\Delta x} c_i(v^n)(w_i^n - w_{i-1}^n)$, one obtains

$$\begin{aligned} v_i^{n+1} - w_i^{n+1} &= (v_i^n - w_i^n) \left(1 + \frac{\Delta t}{\Delta x} c_i(v^n) \right) + \frac{\Delta t}{\Delta x} (c_i(v^n) - c_i(w^n)) (w_i^n - w_{i-1}^n) \\ &\quad - \frac{\Delta t}{\Delta x} c_i(v^n)(v_{i-1}^n - w_{i-1}^n) \end{aligned}$$

Since $c_i(v^n) < 0$ and $v_{i-1}^n \geq w_{i-1}^n$, we get

$$\begin{aligned} v_i^{n+1} - w_i^{n+1} &\geq (v_i^n - w_i^n) \left(1 + \frac{\Delta t}{\Delta x} c_i(v^n) \right) + \frac{\Delta t}{\Delta x} (c_i(v^n) - c_i(w^n)) (w_i^n - w_{i-1}^n) \\ &\geq (v_i^n - w_i^n) \left(1 + \frac{\Delta t}{\Delta x} c_i(v^n) - M^n(w) \Delta t \right) \\ &\geq 0 \end{aligned}$$

$$\text{if } \frac{\Delta t}{\Delta x} \leq \left(2 \sup_{j \in \mathbb{Z}} |c_j(u^n)| \right)^{-1} \text{ and } M^n(v) \Delta t \leq \frac{1}{2}.$$

Case 3: We assume that $c_i(v^n) \geq 0$ and $c_i(w^n) < 0$.

We compute

$$\begin{aligned} v_i^{n+1} - w_i^{n+1} &= v_i^n - w_i^n + \frac{\Delta t}{\Delta x} c_i(v^n)(v_{i+1}^n - v_i^n) - \frac{\Delta t}{\Delta x} c_i(w^n)(w_i^n - w_{i-1}^n) \\ &\geq v_i^n - w_i^n \end{aligned}$$

because $v_{i+1}^n - v_i^n \geq 0$ and $w_i^n - w_{i-1}^n \geq 0$. It is then sufficient to assume that

$$\Delta t \leq \left(\sup_{j \in \mathbb{Z}} \frac{|c_{j+1}(v^k) - c_j(v^k)|}{\Delta x} \right)^{-1} \quad \text{for } 0 \leq k \leq n \quad (28)$$

$$\text{and } \Delta t \leq \left(\sup_{j \in \mathbb{Z}} \frac{|c_{j+1}(w^k) - c_j(w^k)|}{\Delta x} \right)^{-1} \quad \text{for } 0 \leq k \leq n \quad (29)$$

to guarantee the monotonicity of v and the monotonicity of w using Lemma 3.1.

Case 4: We assume that $c_i(v^n) < 0$ and $c_i(w^n) \geq 0$.

We compute

$$v_i^{n+1} - w_i^{n+1} = v_i^n - w_i^n + \frac{\Delta t}{\Delta x} c_i(v^n)(v_i^n - v_{i-1}^n) - \frac{\Delta t}{\Delta x} c_i(w^n)(w_i^n - w_{i-1}^n).$$

But

$$\begin{aligned} 0 &> c_i(v^n) - c_i(w^n) \\ &= -(v_i^n - w_i^n) + \sum_l J_l(v_{i-l}^n - w_{i-l}^n) \\ &\geq -(v_i^n - w_i^n) \end{aligned}$$

and for general $c_+ \geq 0$, $c_- \leq 0$ and $a, b \geq 0$ we have

$$|c_- a - c_+ b| \leq \max(a, b) |c_+ - c_-|$$

and then

$$\begin{aligned} |c_i(v^n)(v_i^n - v_{i-1}^n) - c_i(w^n)(w_{i+1}^n - w_{i+1}^n)| &\leq \Delta x \max(M^n(v), M^n(w)) |c_i(v^n) - c_i(w^n)| \\ &\leq \Delta x \max(M^n(v), M^n(w)) (v_i^n - w_i^n) \end{aligned}$$

Therefore

$$\begin{aligned} v_i^{n+1} - w_i^n &\geq (v_i^n - w_i^n)(1 - \Delta t \max(M^n(v), M^n(w))) \\ &\geq 0 \end{aligned}$$

if we assume $\Delta t \max(M^n(v), M^n(w)) \leq 1$ and (28)-(29).

□

4 Computation of the effective hamiltonian for equation (1)

We recall here that the effective hamiltonian is given in Definition 1.1. Numerically we compute $\bar{H}(A, p)$ for

$$p = \frac{P}{Q} \quad \text{for a fixed } Q \in \mathbb{N} \setminus \{0\} \quad \text{and } P \in \mathbb{Z} \quad (30)$$

Because p is given by (30), we know that the solution w to (1) with initial value given by $w(x, 0) = px$ satisfies

$$w(x + Q, t) = w(x, t) + P.$$

For this reason, numerically we restrict the computation on the interval $\left[-\frac{Q}{2}, \frac{Q}{2}\right]$ with periodic boundary conditions for $\bar{w}(x, t) = w(x, t) - px$ and we write the equation for \bar{w} . In particular we also choose Δx such that $\frac{Q}{\Delta x} \in \mathbb{N} \setminus \{0\}$.

We then use the numerical scheme of Theorem 1.2 with Δt satisfying the CFL conditions stated in Theorem 1.2, which guarantees the monotonicity of the scheme.

4.1 The method to compute the effective hamiltonian

Here we describe two possible strategies to compute numerically the effective hamiltonian $\bar{H}^{\text{num}}(A, p)$.

Method 1: Using the numerical solution w^n of (7), we take its values at two discrete times $t_1 > 0$ and $t_2 > 0$ at a discrete point x_{ref} and we define $\bar{H}^{\text{num}}(A, p) = \frac{v(x_{\text{ref}}, t_2) - v(x_{\text{ref}}, t_1)}{t_2 - t_1}$ for $t_2 - t_1$ large enough, which is difficult to fix in practice.

Method 2: We follow the position of a dislocation (as a marker) starting from a point x_{ref} at time t_1 and waiting until it passes a second time (in the "periodic" interval $[-Q/2, Q/2]$) at the same point at time t_2 , and we define $\bar{H}^{\text{num}}(A, p) = \frac{|P|}{t_2 - t_1}$ with $p = \frac{P}{Q}$ (see Figure 1).

Here $\frac{\bar{H}^{\text{num}}(A, p)}{p}$ can be interpreted as an effective velocity.

In practice we prefer to use the Method 2 in general, because, given a time t_1 large enough, it provides naturally a time t_2 . On the contrary, the result given by the Method 1 can be more sensitive to the choice of t_2 with respect to t_1 .

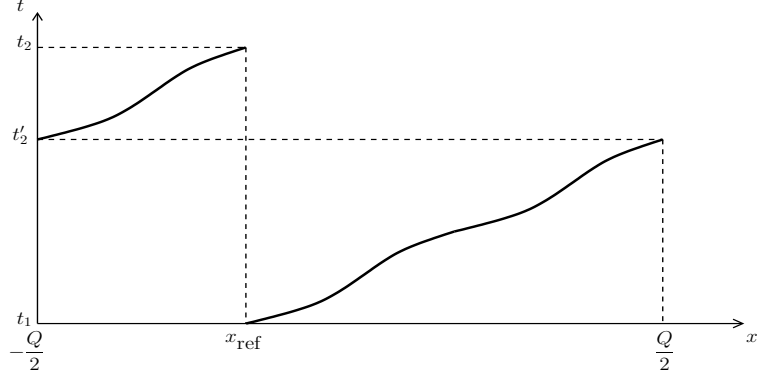


Figure 1: Tracking the trajectory of a dislocation until it comes back to the initial position

4.2 Results of the numerical simulations

Let us recall that the convolution is written as

$$\begin{aligned}
 c^0 \star_{\mathbb{R}} w &= c^0 \star_{\mathbb{R}} (w - px) \\
 &= -\bar{w} + J \star_{\mathbb{R}} \bar{w} \\
 &= -\bar{w} + J^* \star_{[-\frac{Q}{2}, \frac{Q}{2})} \bar{w}
 \end{aligned} \tag{31}$$

with

$$J^*(x) = \sum_{k \in \mathbb{Z}} J(x + kQ). \tag{32}$$

For the present simulations we choose

$$J^*(x) = \frac{1}{Q} \quad \text{for } x \in \left[-\frac{Q}{2}, \frac{Q}{2}\right). \tag{33}$$

We choose

$$c^1(x) = B \sin(2\pi kx) \quad \text{with } k \in \mathbb{N} \setminus \{0\}. \tag{34}$$

For the simulations we have the following particular choices.

Figure	2	3	4	5	6	7	8
c^0	$-\delta_0 + J$	$-\delta_0 + J$	$-\delta_0 + J$	$-\delta_0 + J$	$-\delta_0 + J$	$-\delta_0 + J$	$-\delta_0 + J$
p	0.3125	$(0, 10)$	$2.5/k, k = 1, 2, 3, 4$	$(-10, 10)$	$(-10, 10)$	3	3
A	$(-10, 10)$	$B/k, k = 1, 2, 3, 4$	$(0, 10)$	$(-10, 10)$	$(-10, 10)$	2	2
B	1	1	1	1	1	0	2
k	1	1	1	1	1	2	2
Q	10	10	10	10	10	1	1
Δx	0.01	0.01	0.01	0.01	0.01	0.01	0.01
Δt	$< 10^{-3}$	$< 10^{-3}$	$< 10^{-3}$	$< 10^{-3}$	$< 10^{-3}$	$2.49 \cdot 10^{-3}$	$1.24 \cdot 10^{-3}$
t_1	10	10	10	10	10	-	-

Figure	9	10	11	13	14	16
c^0	$-\delta_0 + J$	$-\delta_0 + J$	(36)	$-\delta_0 + J$	(36)	(39)
p	3	$2.5/k, k = 1, 2, 3, 4$	1, 2, 5, 10	(0.1, 2)	1, 2, 3, 4	0.2, 0.4, 0.7
A	2.5	(0, 10)	(0, 10)	(0, 10)	(0, 10)	(0, 10)
B	2	1	1	-	-	-
k	1	1	1	-	-	-
Q	1	10	10	10	10	10
Δx	0.01	0.01	0.01	0.01	0.01	0.01
Δt	$1.11 \cdot 10^{-3}$	$< 10^{-3}$	$< 10^{-3}$	$< 10^{-4}$	$< 10^{-4}$	$< 10^{-4}$
t_1	-	50	50	$1000\Delta t$	50	50

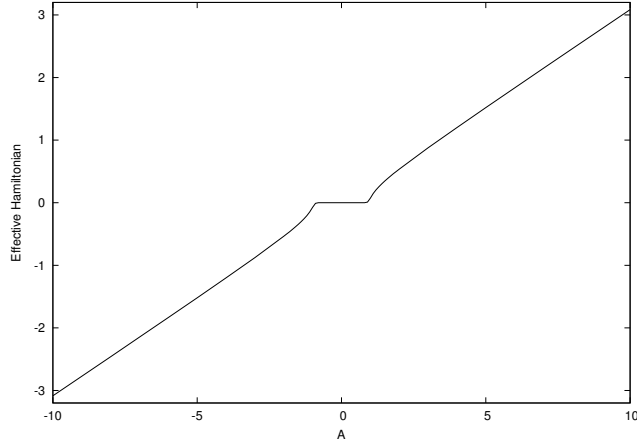


Figure 2: $\bar{H}^{\text{num}}(A, p)$ for $p = 0.3125$ and a monotone kernel $c^0 = -\delta_0 + J$

In Figure 2, we present the numerical effective hamiltonian $\bar{H}^{\text{num}}(A, p)$ which is monotone in A as expected from the first property of Theorem 1.1. Moreover this reveals the existence of a threshold effect, *i.e.* the effective hamiltonian is zero on a whole interval of the parameter A . In addition $\bar{H}^{\text{num}}(A, p)$ is antisymmetric in A because of the symmetries of c^1 . For $|A| \gg B = 1$, the effective hamiltonian is linear and can be approximated here by Ap which is the classical Orowan law (see [13]). In addition, we note that $\bar{H}^{\text{num}}(A, p)$ behaves like the square-root function of A in a neighborhood of the zero-plateau of \bar{H}^{num} .

In Figure 3, the effective hamiltonian $\bar{H}^{\text{num}}(A, p)$ is represented as a function of p for some values of A . We note here the monotonicity of \bar{H}^{num} with respect to p . For a large density of dislocations, the effective hamiltonian \bar{H}^{num} is linear and can again be approximated by Ap .

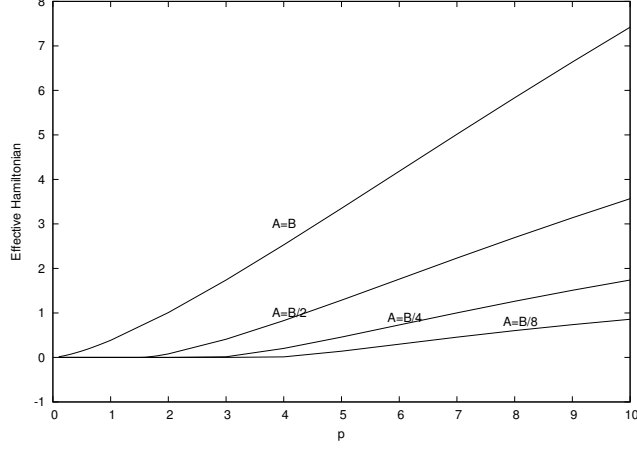


Figure 3: $\bar{H}^{\text{num}}(A, p)$ as a function of the density p for a monotone kernel $c^0 = -\delta_0 + J$

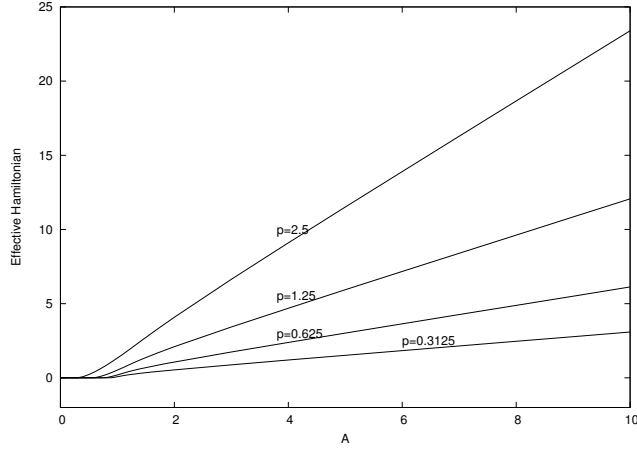


Figure 4: $\bar{H}^{\text{num}}(A, p)$ as a function of A and a monotone kernel $c^0 = -\delta_0 + J$

In Figure 4, we present the effective hamiltonian $\bar{H}^{\text{num}}(A, p)$ as a function of A for several densities of dislocations p . Again we check numerically the qualitative properties of the effective hamiltonian.

In Figure 5, is represented the graph of the effective Hamiltonian \bar{H}^{num} . The X-axis (respectively Y-axis and Z-axis) corresponds to the density of dislocations p (respectively the parameter A and the effective Hamiltonian \bar{H}^{num}). The projection of this graph on the plane (A, p) gives Figure 6 where are represented the level sets of \bar{H}^{num} .

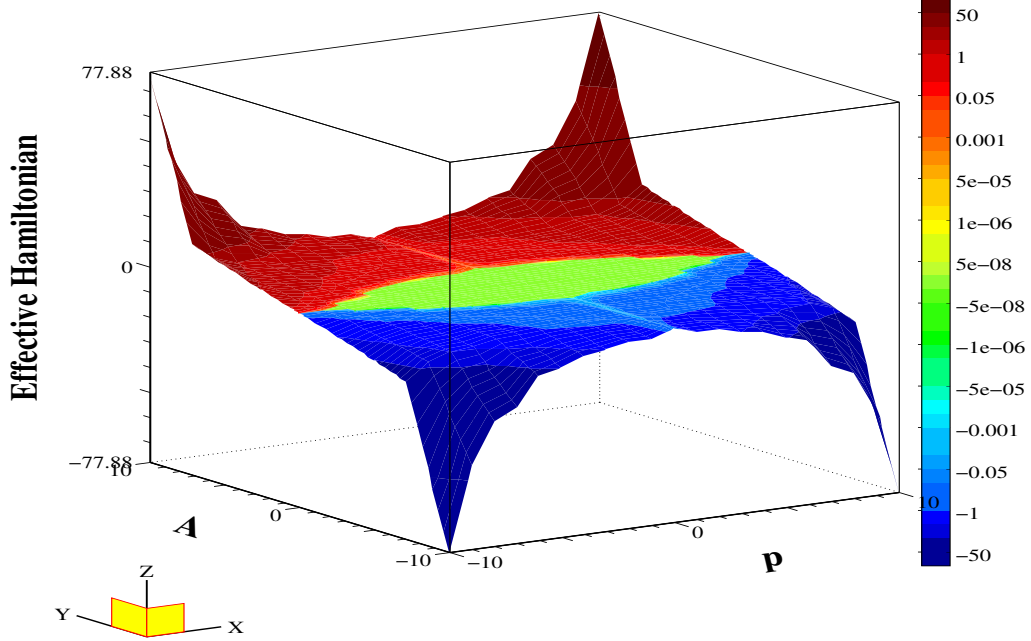


Figure 5: Graph of $\bar{H}^{\text{num}}(A, p)$ for monotone kernel $c^0 = -\delta_0 + J$

In Figure 6, the central region is the set where there is a pinning of the dislocations on the defects represented by the field c^1 , *i.e.* where the effective hamiltonian vanishes. Moreover the monotonicity of \bar{H}^{num} in p reveals that in this model, the ability of the dislocations to pass the obstacles, is increased when we increase the density of dislocations. This is typically a collective behaviour.

5 Computation of the effective hamiltonian for other equations

In this section we study numerically the effective hamiltonian for models where in equation (1) the non-local velocity $c^{\text{int}}[u]$ is replaced by

$$c^{\text{int}}[u] = c^0 \star [u] \quad (35)$$

where $\lfloor \cdot \rfloor$ is the floor function.

Here the positions of dislocations are given by the jumps of $\lfloor u \rfloor$ (see [9]). Let us mention that even for monotone kernel c^0 , the theoretical existence of an effective hamiltonian is not known,

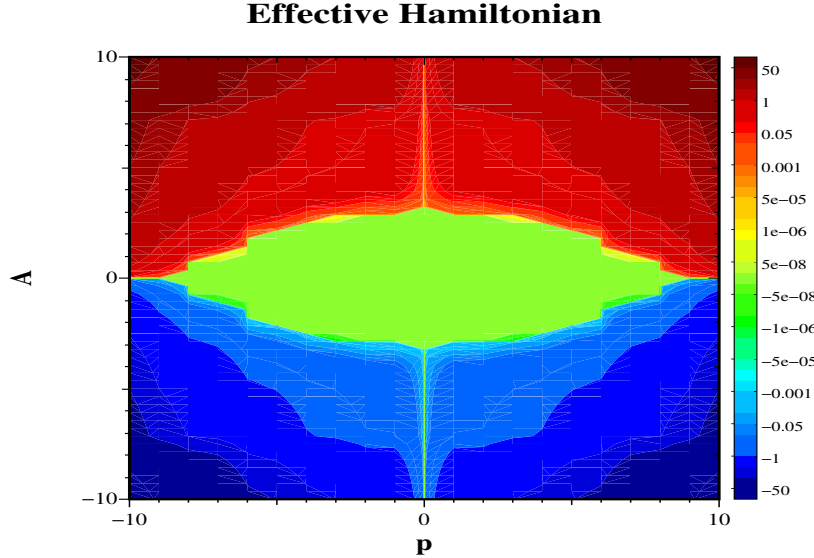


Figure 6: Level sets of the effective hamiltonian $\bar{H}^{\text{num}}(A, p)$

we numerically check that this effective hamiltonian exists in two cases: the monotone kernel (Subsection 5.1) and the Peierls-Nabarro kernel (Subsection 5.2).

5.1 The monotone kernel with one type of dislocations

In this subsection we set $c^0 = -\delta_0 + J$ with $J^* = \frac{1}{Q}$ with the notation of Section 4. This case is strongly related to the homogenization of a Slepčev formulation (see [7]).

First, we represent in Figure 7 the trajectories of 3 dislocations (initially located at $x = -1/3$, $x = 0$, $x = 1/3$) in the case where there are no obstacles (*i.e.* $c^1 = 0$). In this case the trajectories of dislocations are straight lines. A different situation happens (see Figure 8), when we add sufficient obstacles in order to obtain the pinning of dislocations (with $B \geq A$). This case corresponds to the situation where \bar{H}^{num} is equal to zero.

Now, if we increase the parameter A , without changing the obstacles, *i.e.* with the same c^1 , we observe a persistent motion of dislocations (see Figure 9). Numerically, this motion becomes periodic in time. Moreover, we also present in Figure 10 the effective hamiltonian whose behaviour is similar to the case of Section 4.

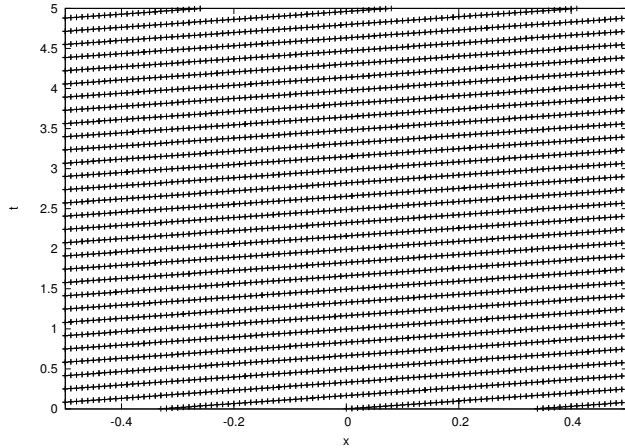


Figure 7: Linear trajectories

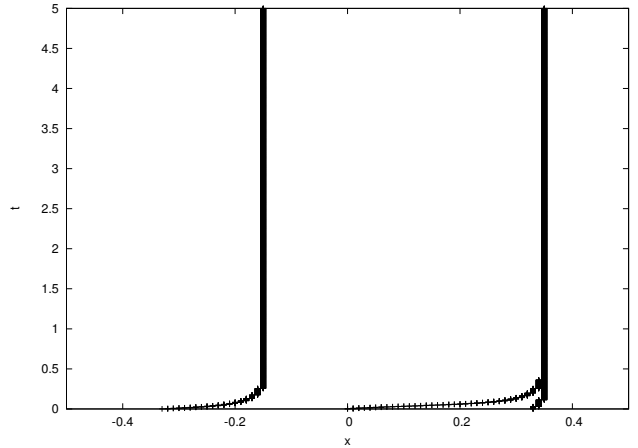


Figure 8: Pinning of dislocations

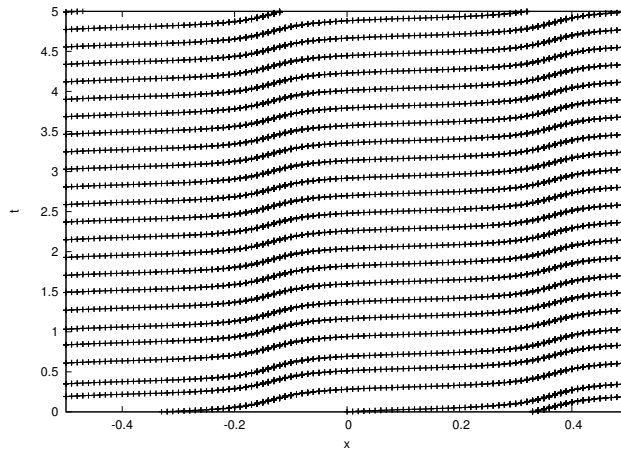


Figure 9: The motion of the dislocations becomes periodic in time

5.2 The Peierls-Nabarro kernel with one type of edge dislocations

In this subsection, we consider the Peierls-Nabarro kernel (see [11, 2]) given by

$$c^0(x) = \frac{-\mu |\vec{b}|^2}{2\pi(1-\nu)} \frac{x^2 - \zeta^2}{(x^2 + \zeta^2)^2} . \quad (36)$$

where $\nu = \frac{\lambda}{2(\lambda + \mu)}$ is the Poisson ratio and λ and $\mu > 0$ are the Lamé coefficients for isotropic

elasticity and \vec{b} is the Burgers vector. We choose $\frac{\mu |\vec{b}|^2}{2\pi(1-\nu)} = 1$ and $\zeta = 0.01$ for our simulations.

Again we compute the effective hamiltonian in Figure 11 which turns out to provide a behaviour similar to the one of Section 4.

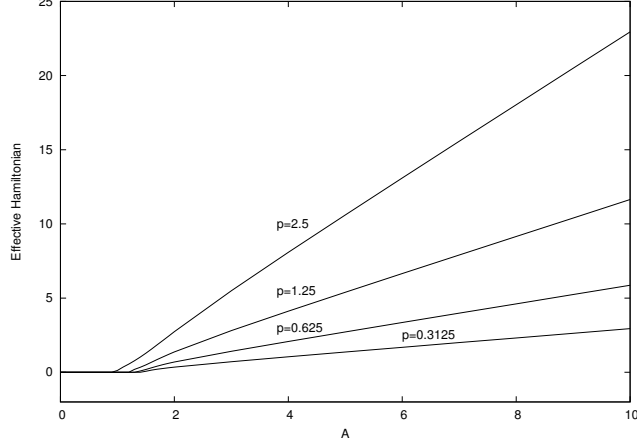


Figure 10: Effective hamiltonian $\bar{H}^{\text{num}}(A, p)$ as a function of A for $c^0 \star \lfloor u \rfloor$, $c^0 = -\delta_0 + J$

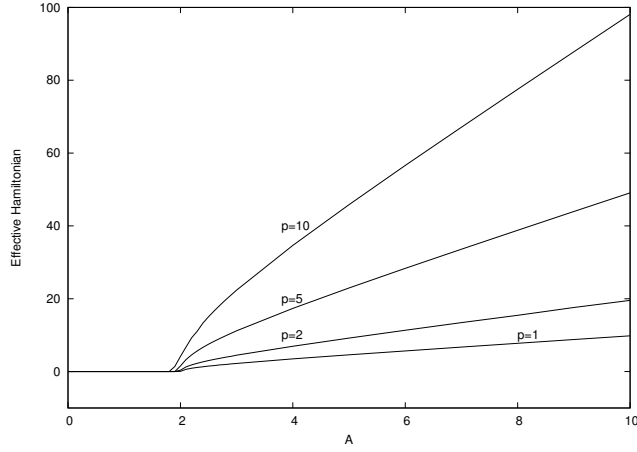


Figure 11: Graph of $\bar{H}^{\text{num}}(A, p)$ for Peierls-Nabarro model with one type of edge dislocations

6 Computation of the effective hamiltonian for systems of equations

In this section, we consider systems of equations describing the motion of dislocations of opposite Burgers vector $(+\vec{b})$ and $(-\vec{b})$. More precisely we study numerically the following system

$$\begin{cases} \frac{\partial u^+}{\partial t}(x, t) = -c[u^+, u^-](x, t) \left| \frac{\partial u^+}{\partial x}(x, t) \right| & \text{in } \mathbb{R} \times (0, +\infty) \\ \frac{\partial u^-}{\partial t}(x, t) = c[u^+, u^-](x, t) \left| \frac{\partial u^-}{\partial x}(x, t) \right| & \text{in } \mathbb{R} \times (0, +\infty) \\ u^+(x, 0) = p^+ x & \text{on } \mathbb{R} \\ u^-(x, 0) = p^- x & \text{on } \mathbb{R} \end{cases} \quad (37)$$

where

$$c[u^+, u^-](x, t) = A + c^0 \star ([u^+(\cdot, t)] - [u^-(\cdot, t)]) . \quad (38)$$

Here the positions of dislocations of Burgers vector $(+\vec{b})$ (respectively $(-\vec{b})$) are represented by the jumps of $[u^+(\cdot, t)]$ (respectively $[u^-(\cdot, t)]$). The motion is schematically represented on Figure 12.

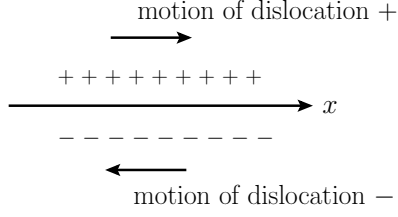


Figure 12: Opposite motion of dislocations + and -

In the following three subsections we will compute the numerical effective hamiltonian for the two types of dislocations $\bar{H}^{\text{num}}(A, p)$ with the same densities $p = p^+ = p^-$ (or the velocity $\frac{\bar{H}^{\text{num}}(A, p)}{p}$) using a numerical method similar to the one used in Sections 4 and 5. We present successively our result in the case of monotone kernel, Peierls-Nabarro kernel for edge dislocations, and the kernel describing the motion of walls of dislocations.

6.1 Monotone kernel

Here we take $c^0 = -\delta_0 + J$ with $J^* = \frac{1}{Q}$ with the notation of Section 4. We present in Figure 13 the effective hamiltonian $\bar{H}^{\text{num}}(A, p)$. We observe a threshold phenomenon, similar to the one of Section 4. Here the dislocations of type - can be seen as obstacles to the motion of the dislocations of type + and vice-versa.

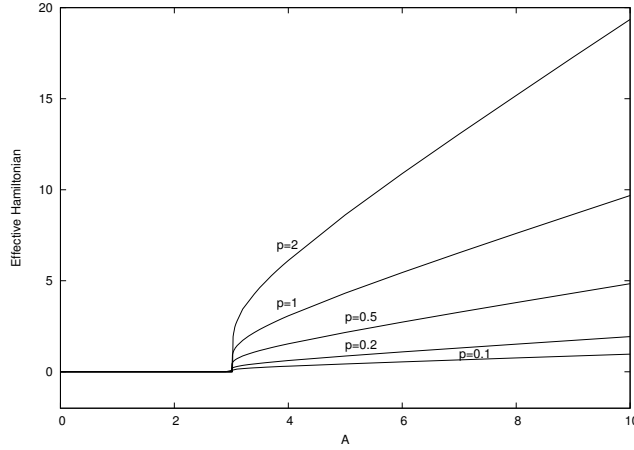


Figure 13: Graph of $\bar{H}^{\text{num}}(A, p)$ as a function of A for $p = p^+ = p^-$ with the monotone kernel

6.2 Peierls-Nabarro kernel for edge dislocations

In this case we take the kernel c^0 given in (36) and the numerical values of Subsection 5.2. We observe in Figure 14 the mean velocity and a threshold effect which increases (apparently linearly) where we increase the density $p = p^+ = p^-$ of dislocations, as physically expected.

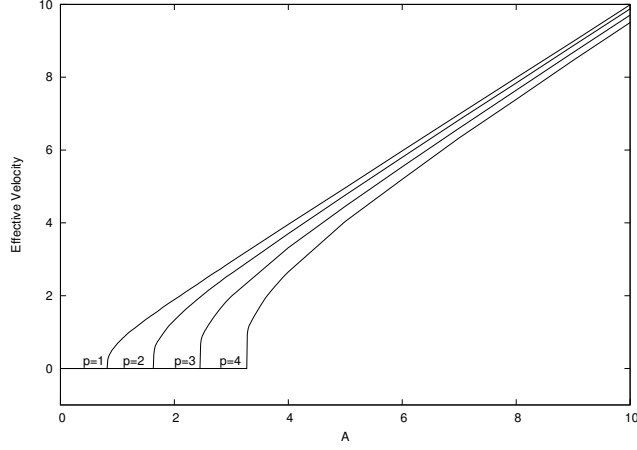


Figure 14: Effective velocity $\frac{\bar{H}^{\text{num}}(A, p)}{p}$ as a function of A for $p = p^+ = p^-$ in the case of Peierls-Nabarro kernel

6.3 Kernel for walls of dislocations

Here we take

$$c^0(x) = \frac{\partial \bar{\sigma}}{\partial x}(x) \quad \text{with} \quad \bar{\sigma}(x) = \frac{\mu |\vec{b}|^2 \pi}{1 - \nu} \frac{\frac{x}{\varepsilon}}{\left(\cosh(2\pi \frac{x}{\varepsilon}) - 1 \right)} \quad (39)$$

with μ is a Lamé coefficient, ν is the Poisson ratio, \vec{b} is the Burgers vector and ε is the distance between dislocations along the y direction (see Figure 15 and the Appendix 7.2).

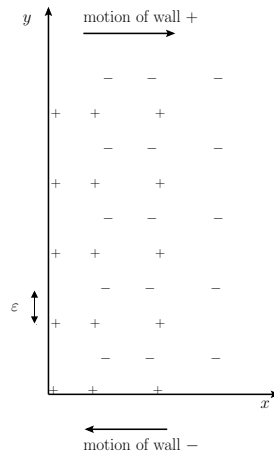


Figure 15: Walls of dislocations + and walls of dislocations -

Here we take $\frac{\mu b^2 \pi}{1 - \nu} = 1$ and $\varepsilon = 1$. We present the effective velocity $\frac{\bar{H}^{\text{num}}(A, p)}{p}$ in Figure 16, and get similar result as in Subsection 6.2 and in [8].

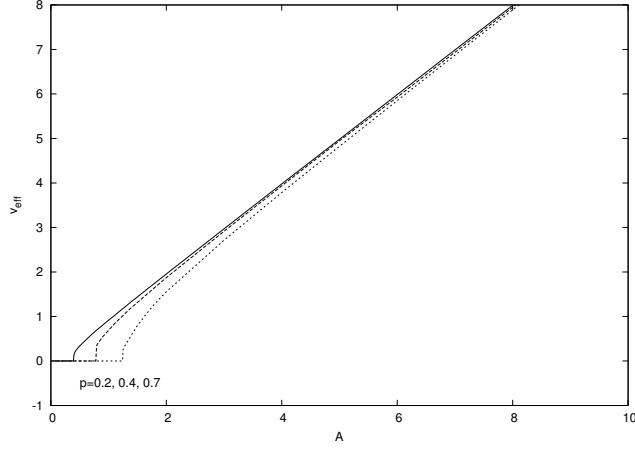


Figure 16: Effective velocity $\frac{\bar{H}^{\text{num}}(A, p)}{p}$ as a function of A for $p = p^+ = p^-$ with the kernel for walls of dislocations

7 Appendix

7.1 Proof of Lemma 2.1

With the notation of Lemma 2.1, we set $c = \frac{Y+y}{2}$ and $\delta = \frac{Y-y}{2} \in \left[-\frac{1}{2}, \frac{1}{2}\right]$. Then we compute

$$\begin{aligned}
(c^0 \star u)(Y) - (c^0 \star u)(Y) &= \int dz J(z) (u(Y+z) - u(Y)) - \int dz J(z) (u(y+z) - u(y)) \\
&= \int d\bar{z} J(\bar{z} - \delta) (u(c + \bar{z}) - u(Y)) - \int d\tilde{z} J(\tilde{z} + \delta) (u(c + \tilde{z}) - u(y)) \\
&\leq - \int dz \inf(J(z - \delta), J(z + \delta)) (u(Y) - u(c + z) + u(c + z) - u(y)) \\
&\leq - (u(Y) - u(y)) c_2
\end{aligned}$$

where we have used the change of variables $\bar{z} = z + \delta$, $\tilde{z} = z - \delta$ in the second line and used the fact that $u(c + \bar{z}) - u(Y) \leq 0$ and $u(c + \tilde{z}) - u(y) \geq 0$ to get the third line.

7.2 Computation of the kernel for walls of dislocations

We recall (see [11]) the stress created by one dislocation at the origin

$$\sigma_{xy}^0(x, y) = \frac{\mu b}{2\pi(1 - \nu)} \frac{x(x^2 - y^2)}{(x^2 + y^2)^2}. \quad (40)$$

Now the stress created by a wall of dislocations at the positions $x = 0$, $y = k\varepsilon$ for $k \in \mathbb{Z}$ is given by

$$\begin{aligned}
\sigma_{xy}(x, y) &= \sum_{k \in \mathbb{Z}} \sigma_{xy}^0(x, y - k\varepsilon) \\
&= \frac{\mu b \pi}{1 - \nu} \frac{\frac{x}{\varepsilon} (\cosh(2\pi \frac{x}{\varepsilon}) \cos(2\pi \frac{y}{\varepsilon}) - 1)}{\left(\cosh(2\pi \frac{x}{\varepsilon}) - \cos(2\pi \frac{y}{\varepsilon}) \right)^2}. \quad (41)
\end{aligned}$$

(see [11] page 733, formula (19-73)). Then

$$c^0(x) = b \frac{\partial \sigma_{xy}}{\partial x}(x, 0) = \frac{\partial \bar{\sigma}}{\partial x}(x) \quad (42)$$

with $\bar{\sigma}(x) = b \sigma_{xy}(x, 0)$.

Acknowledgements

The authors would like to thank O. Alvarez, M. El Rhabi, A. Finel and Y. Le Bouar for fruitful discussions. This work was supported by the contract JC 1025 called "ACI jeunes chercheuses et jeunes chercheurs" of the French Ministry of Research (2003-2007).

References

- [1] R. Abgrall, *Numerical discretization of boundary conditions for first order Hamilton-Jacobi equations*, SIAM J. Numer. Anal. 41 (6), 2233-2261, 2003.
- [2] O. Alvarez, P. Hoch, Y. Le Bouar and R. Monneau, *Dislocation dynamics: short time existence and uniqueness of the solution*, Arch. Ration. Mech. Anal. 181 (3), 449-504, 2006.
- [3] M. Bardi and I. Capuzzo-Dolcetta, *Optimal Control and Viscosity Solutions of Hamilton-Jacobi-Bellman Equations*, Birkhäuser, Boston, 1997.
- [4] G. Barles, *Solutions de Viscosité des Equations de Hamilton-Jacobi*, Springer-Verlag, Berlin, 1994.
- [5] M.G. Crandall and P.-L. Lions, *Conditions d'unicité pour les solutions généralisées des équations de Hamilton-Jacobi du premier ordre*, C. R. Acad. Sci. Paris Ser. I Math., 292, 183-186, 1981.
- [6] M.G. Crandall, H. Ishii and P.-L. Lions, *User's guide to viscosity solutions of second order partial differential equations*, Bull. Amer. Math. Soc. (N.S.), 27, 1-67, 1992.
- [7] N. Forcadel, C. Imbert and R. Monneau, work in progress.
- [8] A. Ghorbel, M. El Rhabi and R. Monneau, *Comportement mécanique par homogénéisation de la dynamique des dislocations*, Proceedings of Colloque National MECAMAT - Aussois 2006, Ecole de Mécanique des Matériaux - Aussois 2006 (january 2006, Aussois, France).
- [9] A. Ghorbel and R. Monneau, *Well-posedness of a non-local transport equation modelling dislocations dynamics*, preprint Cermics-ENPC 304, 2006.
- [10] D.A. Gomes and A.M. Oberman, *Computing the effective Hamiltonian using a variational approach*, SIAM J. Control Optim. 43 (3), 792-812, 2004.
- [11] J.R. Hirth and L. Lothe, *Theory of dislocations*, Second Edition. Malabar, Florida : Krieger, 1992.
- [12] C. Imbert, R. Monneau and E. Rouy, *Homogenization of first order equations with (u/ε) -periodic Hamiltonians. Part II*, preprint on HAL server of CNRS [ccsd-00080397 - version 1] (28/06/2006).
- [13] J. Kratochvil, R. Selaček and E. Werner, *The importance of being curved: bowing dislocations in a continuum description*, Philos. Mag. 83 (31-34), 3735-3752, 2003.

- [14] P.-L. Lions, G. Papanicolaou and S.R.S. Varadhan, *Homogenization of Hamilton-Jacobi equations*, unpublished preprint, 1986.
- [15] M. Rorro, *An approximation scheme of the effective Hamiltonian and applications*, *Appl. Numer. Math.* 56 (9), 1238-1254, 2006.